Vibration control of flexible structures using fusion of inertial sensors and hyper-stable actuator-sensor pairs

C. Collette [1], **F. Matichard** [2,3]
[1] Université Libre de Bruxelles, BEAMS department,
50 F.D. Roosevelt av., 1050 Brussels (Belgium)
e-mail: **ccollett@ulb.ac.be**

[2] Massachusetts Institute of Technology,
185 Albany St., NW22-295 Cambridge, MA. 02139 (United States)

[3] California Institute of Technology,
1200 East California Boulevard, Pasadena California 91125 (United States)

Abstract
This paper discusses sensor fusion techniques that can be used to increase the control bandwidth and stability of active vibration isolation systems. For this, a low noise inertial instrument dominates the fusion at low frequency to provide vibration isolation. Other types of sensors (relative motion, smaller but noisier inertial, or force sensors) are used at higher frequencies to increase stability. Several sensor fusion configurations are studied. The paper shows the improvement that can be expected for several case studies.

1 Introduction

Active systems are often required to isolate sensitive equipment from input motion disturbance [1, 2]. High performance is often reached by combining high loop gain feedback control and very low noise inertial sensors [3, 4]. In order to have sufficient stability margins, it is common practice is to collocate sensors and actuators [5, 6]. Such feedback systems are sometimes referred to as hyper-stable [7]. However, in practice, several factors can cause phase loss, including analog-to-digital converters, dynamics of sensors and actuators [8], or resonances involving flexibility between the actuator and the sensor [9]. Under these practical constraints, the stability becomes conditional. Even with a careful design, the flexibility between sensors and actuators remains difficult to avoid at high frequency, especially when large and heavy sensors must be used to achieve very low noise isolation performance [10]. Such modes, known as in-the-loop modes [11], are the topic of this paper.

In order to limit the effect of these modes on the stability, a conservative approach is to limit the bandwidth well below the lowest structural natural frequencies. Another option is to damp the resonances passively, e.g. with Dynamic Vibration Absorbers (DVA) [12, 13]. Another possibility is to use the so-called plant inversion and notch filtering techniques [14, 10]. The major drawback of these techniques is that they depend on the knowledge of the system, and thus, they are sensitive to plant variations.

Sensor fusion techniques have been used in active vibration isolators to combine the benefits of different types of sensors. They can combine relative sensor providing DC positioning capability at low frequency with inertial sensors providing isolation at higher frequency [15]. In other applications, they are used to combine inertial sensor at low frequency with force sensor at higher frequency to improve the robustness [16], or damp the internal modes [17, 18]. In this paper, we study and compare different sensor fusion methods combining inertial sensors at low frequency with sensors adding stability at high frequency, including dual configurations [19].

Section two summarizes fundamental features and limitations of feedback control systems using relative motion, force, or inertial sensors independently. Sections three and four investigate different types of high frequency sensor fusions and their impact on the stability of flexible equipment. Section five draws the conclusions.

2 Different types of sensors

Several types of sensors can be used for the feedback control of vibration isolation systems:

- Feedback control based on relative motion sensors (inductive, capactive, ferromagnetic sensors...) typically permits to servo-position a system or platform relative to a reference (e.g. floor or support base), but does not provide isolation from the ground motion.
- Feedback control based on force sensors typically lowers the effective natural frequency, and therefore increases the isolation, but sacrifices the systems compliance in doing so.
- Feedback control based on inertial sensors (geophones, seismometers, accelerometers...) improves not only the vibration isolation but also the compliance. Inertial sensors are, however, AC coupled and noisy at low frequencies.

Inertial sensors are available in a broad variety of size and noise performance. The complexity required to obtain low self-noise at low frequency implies that the more sensitive is the instrument, the larger and heavier it tends to be. This compromise between sensor noise and sensor size has a direct impact on active vibration isolation systems design and their servo-control bandwidth. When low noise performance is needed at low frequencies, large instruments will be preferred.

However, they will put constrains on the design. First, it is harder to maintain collocation between sensors and actuators over large bandwidth when large and heavy sensors are used. This has a direct impact on the achievable control bandwidth, as discussed in the next sections. Then, the size and weight of sensors will put constrains on the platform's design. The rigidity of the structure and the modal content have a direct influence on the servo-controller bandwidth. The stiffer the structure, the easier it is to achieve high control bandwidth. Compared to smaller instruments, large and heavy sensors will tend to lower the structures natural frequencies, and therefore indirectly reduce the control bandwidth. Consequently, there is a subtle compromise to be obtained between sensor noise and the influence of the sensor size on the system's design and on the control bandwidth.

In the next sections, we study the combination of several types of sensors, to obtain both broadband low noise sensing and high bandwidth. The signal from the inertial sensor is used at low frequency. It is filtered by a low-pass filter L_p. The signal providing high-frequency stability is filtered by a high-pass filter H_p. The filters L_p and H_p are chosen to be complementary filters [15] to simplify the control loops design, i.e. $L_p + H_p = 1$. The numerical values of the filters used in this paper are

$$L_p = \frac{334867788.1472(s^2 + 213.3s + 2.274e004)}{(s + 377)(s^2 + 380.3s + 9.389e004)(s^2 + 575.6s + 2.151e005)}$$

$$H_p = \frac{s^3(s^2 + 1333s + 8.883e005)}{(s + 377)(s^2 + 380.3s + 9.389e004)(s^2 + 575.6s + 2.151e005)}$$

These filters will be used throughout the paper. The crossing frequency of the complementary filters is set slightly above the unity frequency of the controllers used in the next sections. Far from the crossing frequency, the filters asymptote to a third-order cut-off to ensure the inertial sensor signal dominates at low frequency, and the newly introduced sensor dominates at high frequency where we expect to improve performance.

Three types of sensors are studied to improve the high frequency stability: (i) a smaller inertial sensor (e.g. a piezoelectric accelerometer), noisier at low frequency but easier to collocate with the actuator; (ii) a relative motion sensor dual of the actuator (hyperstable); (iii) a force sensor (also dual with the actuator/hyperstable).

In order to get a good physical insight, these three possibilities of high-frequency fusion will be studied on models with an increasing level of complexity.

3 Inertial control and sensor fusion configurations

While this paper addresses the problem of feedback control stability inherent to flexible structure models, this section uses a one degree of freedom model to introduce control and fusion techniques that will be used on flexible structures in the next sections. In this section, standard inertial-sensor-only control is discussed first for reference, and then the inertial sensor is fused with each sensor type to demonstrate the impact on transmissibility and compliance.

3.1 Controller based on inertial sensing

Figure 1(a) shows the simplest model of an infinitely rigid and suspended structure, represented by a single degree of freedom (d.o.f.) isolator.

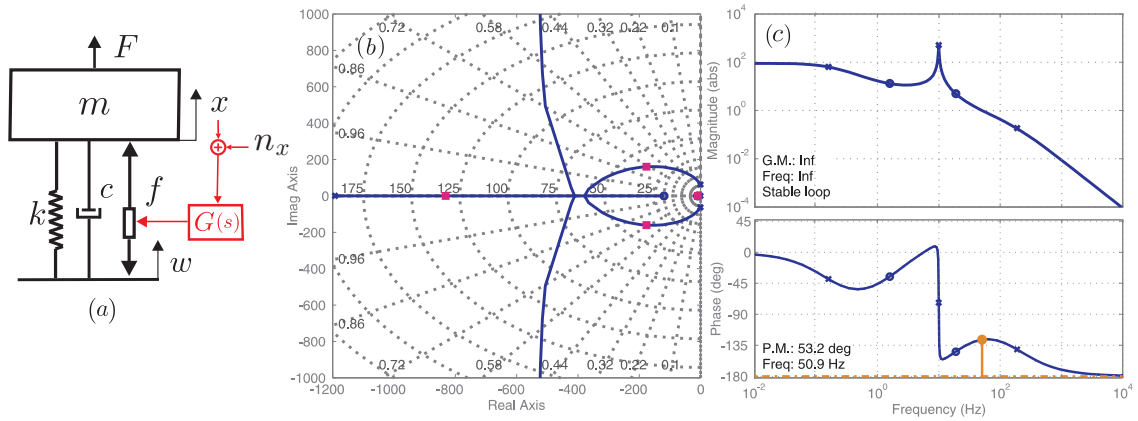

Figure 1: (a) Single d.o.f. isolator with inertial control; (b) Root locus and (c) Open loop transfer function.

The dynamics of the system reads

$$(ms^2 + k)x = kw + f \tag{1}$$

where m is the mass of the equipment, k is the stiffness of the suspension, w is the motion of the ground and f is the control force. The absolute motion of the mass, x, is measured with an inertial sensor, considered as perfect (i.e. without internal dynamics and its velocity signal is integrated and calibrated into displacement units). It is important to point out that inertial sensors are inherently AC coupled which typically results in a lower unity gain frequency in the control loop. Fusion techniques can be used at low frequency to deal with this problem [15]. However, these low frequency issues and techniques are not discussed here to avoid confusion with the fusion techniques discussed later (to increase the high frequency stability). Therefore, the AC coupling nature of the inertial sensor is not represented in the following transfer functions. It is assumed that the inertial sensor transfer function has been perfectly stretched (inverted/integrated) down to the lowest frequency studied (10 mHz). The control force is driven by this perfectly calibrated inertial motion measurement through the compensator:

$$f = -G(s)(x + n_x) = -gH(s)(x + n_x) \tag{2}$$

where n_x is the inertial sensor noise also calibrated in displacement units. The mechanical system's parameters are defined as follows to illustrate the discussion: $m = 300\ kg$, $10\ Hz$ natural frequency, and $1\ \%$ of critical damping ($k = 1.18\ MN/m$ and $c = 0.02\sqrt{km} = 377\ Ns/m$)[1]. A typical controller is defined to support the discussion. It is composed of a lag to increase the loop gain at low frequency, a lead to have a sufficient phase margin at high frequency, and a gain value of $g = 9k$ has been chosen to set appropriate unity gain frequency just above $50\ Hz$:

$$G(s) = gH(s) = 9k\frac{10(s + 119.2)(s + 10)}{(s + 1192)(s + 1)} \tag{3}$$

Figure 1(b) and (c) shows the corresponding root locus and open loop transfer function (Gx/f) of this system. Substituting Equ. (2) in Equ. (1) gives:

$$x = \frac{k}{(ms^2 + k + G)}w + \frac{1}{(ms^2 + k + G)}F - \frac{G}{(ms^2 + k + G)}n_x \tag{4}$$

The isolator's transmissibility (x/w) and compliance (x/F) are shown in Figs. 2 (a) and (b). They illustrate

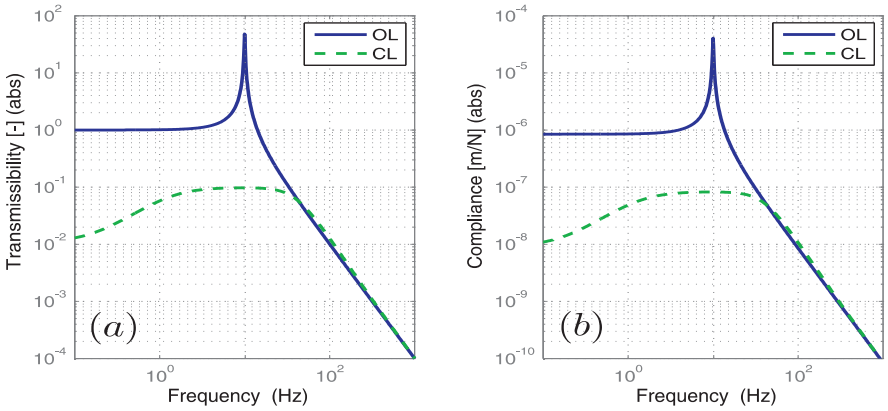

Figure 2: (a) Transmissibility and (b) compliance of a single d.o.f. isolator in Open Loop (OL) and Closed Loop (CL) configuration.

that the controller based on inertial sensing improves not only the compliance but also the transmissibility.

3.2 Inertial and force sensor

A force sensor mounted between the suspended mass and the active suspension exhibits hyper-stability properties [6]. In this section we discuss the fusion of the inertial sensor signal with a force sensor using the same one d.o.f. model. The force sensor collocated with the actuator is mounted as shown in Fig. 3(a). The inertial sensor (large and heavy, but very sensitive) is used at low frequency where isolation performance is needed. The force sensor F_a (noisier but forming a dual pair with the actuator) is used at higher frequency to improve the stability.

[1] Experience shows that structures embedding heavy, low-frequency, low-noise instrumentation typically weighs several hundreds of kg to several tons. We picked the number $300\ kg$ to illustrate the order of magnitude of the mass of such structures (a single, broadband, three-axis seismometer weighs roughly $15\ kg$). We picked an intermediate fundamental resonance value of $10\ Hz$, between soft suspensions isolators frequencies (around a $1\ Hz$ or below) and stiff suspensions frequencies (around several tens of Hertz). Other values could have been arbitrarily picked and lead to the same conclusion as in the simulation presented in the next section to illustrate the various sensor fusion methods.

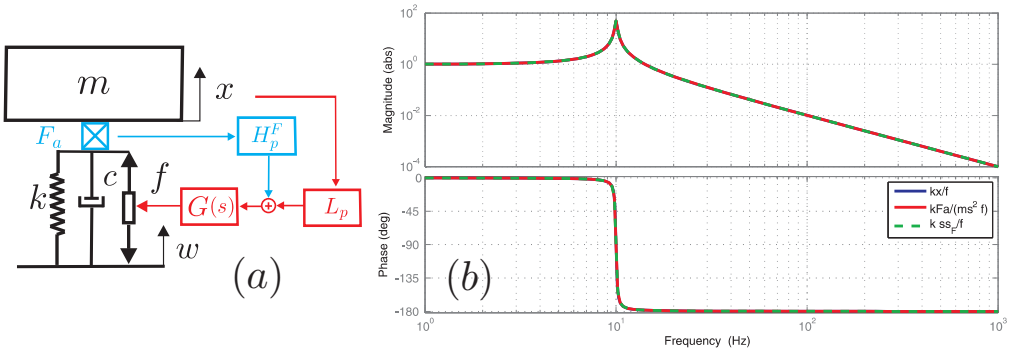

Figure 3: (a) Single d.o.f. isolator. Inertial and force control fusion; (b) Open loop transfer function kx/f, $kF_a/(ms^2 f)$ and kss_F/f.

In this case, the control force is

$$f = -G(s)ss_F = -gH(s)ss_F \tag{5}$$

where ss_F is called a *super sensor*, constructed from the fusion of the inertial sensor and the force sensor:

$$ss_F = L_p(x + n_x) + H_p^F(F_a + n_F) \tag{6}$$

where n_x and n_F are respectively the noise in the inertial sensor and the noise in the force sensor, calibrated in displacement and force units respectively, and

$$H_p^F = \frac{H_p}{ms^2} \tag{7}$$

is a filter combining the high pass complementary filter H_p and a calibration factor to match the unit of the force sensor and inertial sensor (assumed to be in displacement units all along the text), where L_p and H_p are complementary filters shown in section 2.

Figure 3(b) shows the open loop transfer function between the actuator f and the super sensor ss_F. It is normalized by the stiffness k for readability.

Replacing Equs.(6) and (5) in (1), we get

$$x = \frac{k}{ms^2 + k + G}w + \frac{1 + GH_p^F}{ms^2 + k + G}F - \frac{G(L_p n_x + H_p^F n_F)}{ms^2 + k + G} \tag{8}$$

The first term on the right hand side of (8) shows that the transmissibility is unchanged (by comparison with the inertial control). The second term shows that the compliance is degraded by a factor $(1 + GH_p^F)$. The third term shows the noise introduced by the force sensor. As an illustration, Fig. 4 shows the resulting closed loop transmissibility and compliance obtained using the controller defined in Equ.(3). The curves have been obtained with the same value of g as before. The fusion filter can then be adjusted as a function of the application objectives to obtain a good compromise between sensor noise filtering and compliance degradation. (i.e. more slope at low frequency in H_p for better force sensor noise filtering would result in more amplification near the complementary filters crossover frequency).

3.3 Inertial and relative sensor

Control based on relative motion sensor tends to reduce the vibration isolation. However, this sensor form a dual pair with the actuator when both are collocated. Therefore, a sensor fusion can be implemented using the

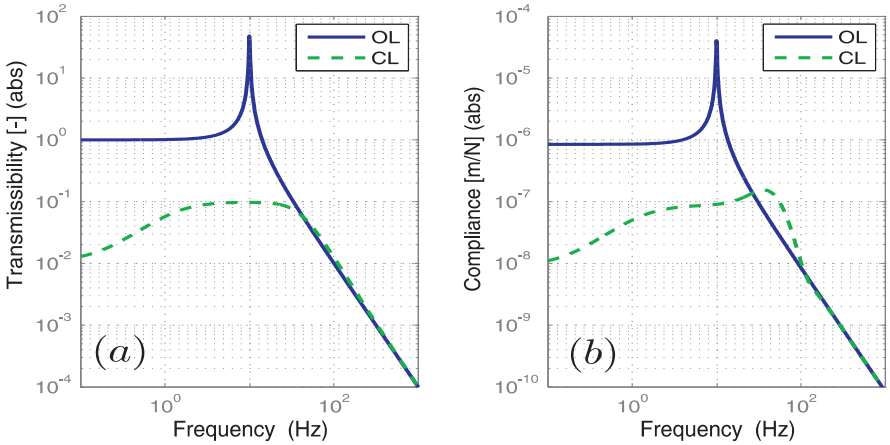

Figure 4: Inertial sensor blended with a force sensor. (a) Transmissibility and (b) compliance of a single d.o.f. isolator in Open Loop (OL) and Closed Loop (CL) configuration.

inertial sensor at low frequency (to provide isolation) and using the relative motion sensor at high frequency (to improve stability). The relative motion sensor is collocated with the actuator, as illustrated in Fig. 5(a).

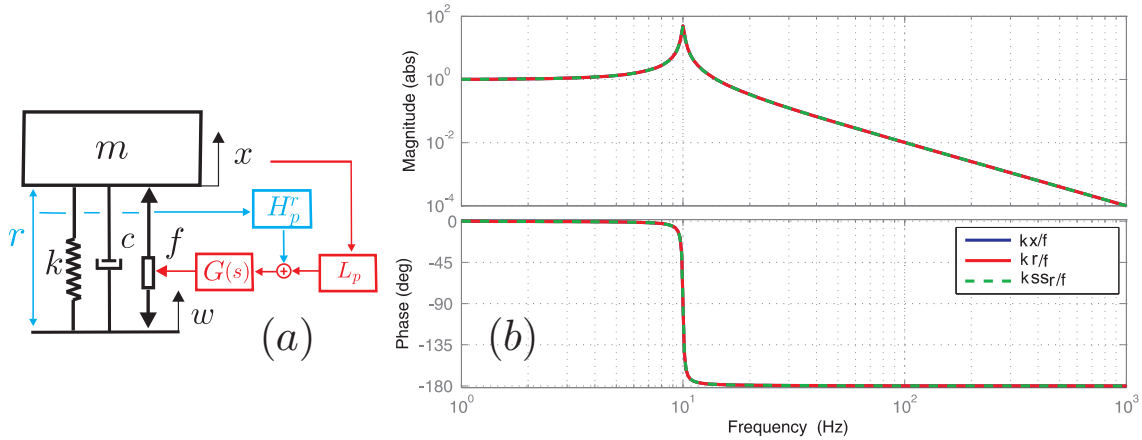

Figure 5: (a) Single d.o.f. isolator. Blend of an inertial sensor and a relative motion sensor; (b) Open loop transfer function kx/f, kr/f and kss_r/f.

In this case, Equ.(2) becomes

$$f = -Gss_r = -gH(s)ss_r \tag{9}$$

where

$$ss_r = L_p(x + n_x) + H_p^r(r + n_r) \tag{10}$$

where r is the relative motion sensor and n_r is its intrinsic noise, calibrated in displacement units. Figure 5(b) shows the open loop transfer function between the actuator f and the super sensor ss_r.

Replacing Equs.(10) and (9) in (1), we get

$$x = \frac{k + GH_p^r}{ms^2 + k + G}w + \frac{1}{ms^2 + k + G}F - \frac{G(L_p n_x + H_p^r n_r)}{ms^2 + k + G} \tag{11}$$

in which the fractions of the right hand side are respectively the transmissibility, the compliance and the noise sensitivity. Compared to Equ.(4), one can be notice that there is a significant degradation of the isolation at high frequency, because the relative sensor couples both sides of the actuator, while the compliance remains

unchanged. The third term shows the noise introduced by the relative sensor. Figure 6 shows the resulting closed loop transmissibility and compliance. The curves have been obtained with the same value of g as before.

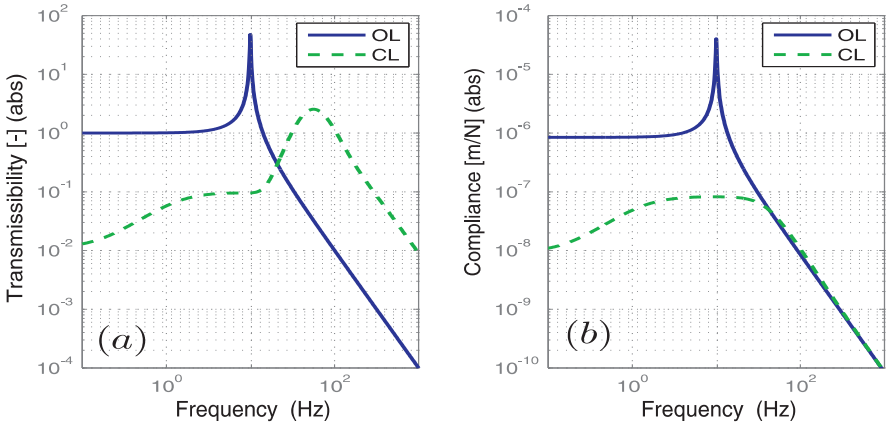

Figure 6: Inertial sensor blended with a relative motion sensor. (a) Transmissibility and (b) compliance of a single d.o.f. isolator in Open Loop (OL) and Closed Loop (CL) configuration.

Fusion with a relative motion sensor has no negative effect on the compliance, unlike fusion with a force sensor (Fig.4(b)). However, compared to Fig.4(a), the transmissibility shown in Fig.6(a) has been degraded, due to the coupling introduced by the relative motion sensor. The blend filters can be tuned to change the compromise between isolation in the bandwidth and amplification outside. Nevertheless, this example illustrates the overall tendency. This approach can be of interest for systems using stiff suspensions and therefore providing little passive isolation, although the flexibility of the support structure must be carefully taken into account for the design of the blend filters.

In the next section, we will study the effect of the structure deformation on these sensor fusion methods. For that, a storage element (modeled by a spring) is introduced between the actuator and the sensor to study the stability of the feedback loop.

4 Flexible structure

With structural flexibility between the inertial sensor and actuator, the open loop gain transfer function can lose its hyper-stable properties with the same controller. In this section, we follow the same examples as in section 3, but now including an additional degree of freedom to represent the impact of structure flexibility to demonstrate the impact of sensor fusion.

4.1 Inertial sensor control

A two d.o.f. system shown in Fig. 7(a) is introduced to represent the effect of structure's flexibility. Compared to Fig. 1(a), the mass of the isolator has been divided in two smaller masses, connected by a spring and a dashpot. This two mass system represents the flexibility of the structure between the location of the inertial sensor, and the point on which the actuator applies a force on the structure.

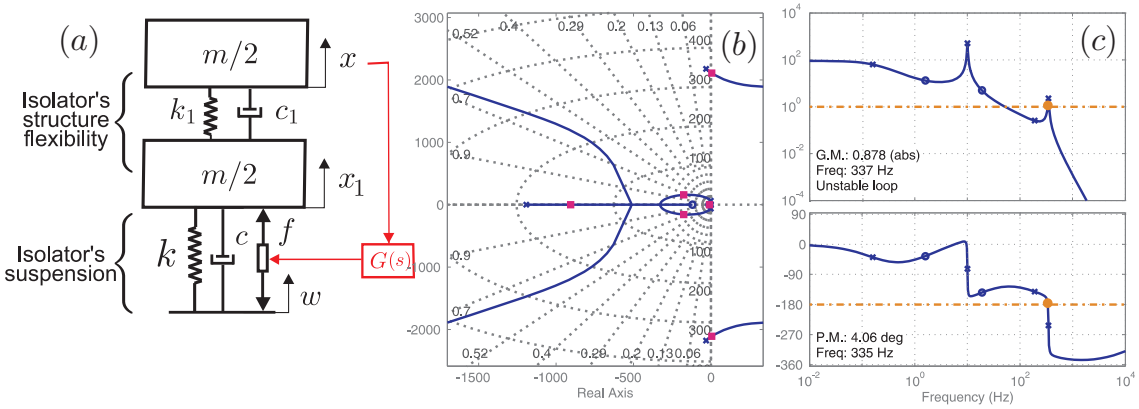

Figure 7: (a) Active isolator model including first structural mode; (b) Root locus and (c) Open loop transfer function with the controller G shown in Equ.(3) on the mass inertial displacement x.

In order to keep the results comparable with the case of the single d.o.f. system, the total mass is kept the same, and equally distributed between the two bodies. The stiffness k and damping ratio of the isolator suspension are unchanged. The model uses a stiffness $k_1 = 300k = 355\ MN/m$, $c_1 = 0.02\sqrt{k_1 m/2} = 4617\ Ns/m$ to be representative of a typical first deformation mode of structure. The control force is still given by Equ.(2). Figures 7(b) and (c) show the root locus and the open loop transfer function between the actuator and the sensor, using the same controller shown in Equ.(3). The system is now unstable, because there is no zero to restore the phase between two resonances. It is a direct consequence of the non-collocated configuration between the actuator and the sensor. The high frequency mode is known as a in-the-loop mode [11]. The system can still be stabilized by tuning the controller, via notching or plant inversion as mentioned in the introduction. However, it is more difficult to obtain a sufficient phase margin, and a good robustness to model parameter variations. Further, this is an illustrative model with only one mode of compliance. Real structures may have many such modes making the control design implementation very complicated. In the next three sections, we will blend the inertial sensor with another inertial sensor mounted closer to the actuator, with a force sensor and with a relative motion sensor. For each case, we will investigate the effect of the blend on the stability of the control loop.

4.2 Inertial and small accelerometer

Mounting a smaller inertial sensor near the actuator and fusing its signals with the distant low-frequency seismometer is one way to regain stability. This is illustrated in Fig.8(a). In this example, the low-frequency inertial sensor (large and heavy) can't be exactly collocated with the actuator. It senses the motion x. A smaller inertial sensor (an accelerometer in this example) is used to sense the absolute motion at the actuation point.

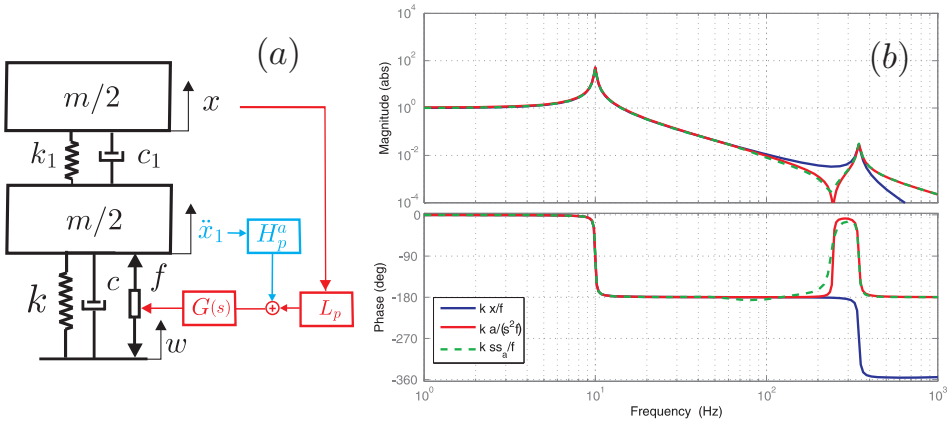

Figure 8: (a) Two d.o.f. isolator. Inertial sensor blended with an accelerometer; (b) Open loop transfer function kx/f, $ka/(s^2 f)$ and kss_a/f.

In this case, Equ.(2) becomes

$$f = -gH(s)ss_a \tag{12}$$

where the super sensor ss_a is constructed from the blending of the inertial sensor x and the accelerometer $a = \ddot{x}_1$:

$$ss_a = L_p x + H_p^a a \tag{13}$$

where $H_p^a = H_p/s^2$ and L_p and H_p are complementary filters shown in section 2. The normalized open loop transfer function kx/f, $ka/(s^2 f)$ and kss_a/f are shown in Fig. 8(b). The main difference between kx/f and kss_a/f is that a pair of zeros appeared in kss_a/f at high frequency (its value corresponds to the resonance of the subsystem where x_1 is restrained). As a result, the phase remains bounded between $0°$ and $-180°$, which means that the use of an inertial sensor near the actuator permits to regain the phase stability. In this example, fusion works very well because the frequency of the zeros is far enough from the blend frequency, i.e. the super sensor ss_a is completely dominated by the accelerometer signal at high frequency. However, this is not a truly dual actuator/sensor configuration. Moreover, the smaller inertial sensors will be noisier than the large inertial sensor used to sense x. It is therefore important to verify that the noise introduced by the small inertial inertial sensor does not compromise the vibration isolator performance (noise or error budgeting).

4.3 Inertial and force sensor

The fusion of the inertial and force sensor presented in section 3.2 is now applied to the flexible structure to illustrate the benefits on loop shaping and stability. The inertial sensor is combined with a force sensor collocated with the actuator, as shown in Fig.9(a).

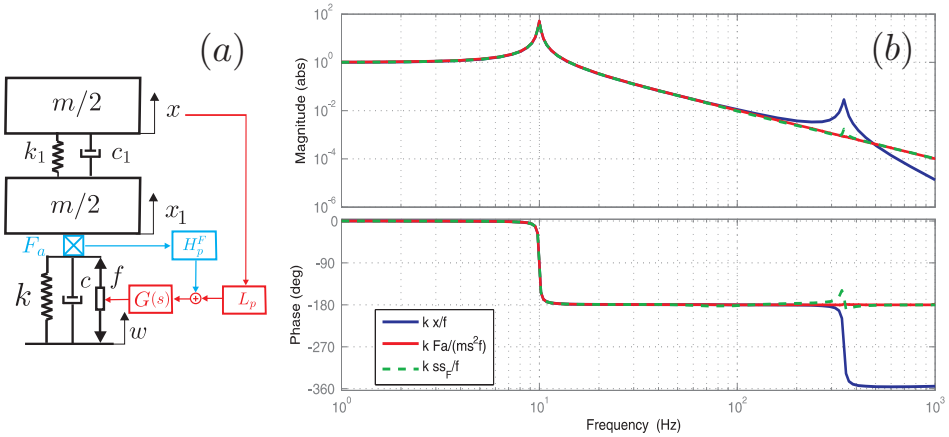

Figure 9: (a) Two d.o.f. isolator representing a flexible structure. Inertial sensor blended with a force sensor; (b) Open loop transfer functions kx/f, $kF_a/(ms^2f)$ and kss_F/f.

The expression of the super sensor ss_F is still given by Equ.(6) and the control force is also still given by Equ.(5)[2]. Figure 9(b) shows the open loop transfer functions kx/f, $kF_a/(ms^2f)$ and kss_F/f. At low frequency, kss_F/f is dominated by the absolute motion sensor; at high frequency, it is dominated by the force sensor. The figure shows that the phase lag stops at $-180°$, because a pair of zeros appeared just before the second pair of poles and cancels the poles. The frequency of the zeros corresponds to the resonance of a subsystem made of the two masses connected by k_1 and c_1 only (not connected to k and c). In this example, the zero nearly cancels the third pole because k is significantly lower than k_1. This example illustrates that this fusion technique simplifies the loop shaping of the controller because the open loop is less sensitive to the deformation mode.

4.4 Inertial and relative sensor

The fusion of the inertial and relative sensor presented in section 3.3 is now applied to the flexible structure to illustrate the benefits on stability. Consider the flexible structure shown in Fig. 10(a), where a relative sensor has been mounted in order to measure the elongation of the actuator.

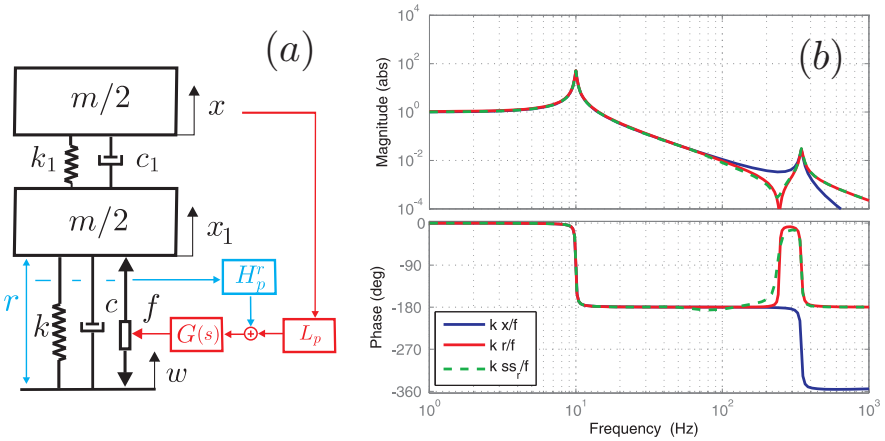

Figure 10: (a) Two d.o.f. isolator representing a flexible structure. Blend of an inertial sensor and a relative motion sensor; (b) Open loop transfer functions kx/f, kr/f and kss_r/f.

[2]In [20, 18], a similar controller has been proposed to damp the equipment modes, while here we are only interested in the controller stability at high frequency.

The control law is still given by Equ.(9), and the super sensor by Equ.(10). Figure 10(b) shows the open loop transfer function kx/f, kr/f and kss_r/f. It can be shown that the relative sensor has introduced a coupling between both sides of the actuator, which induces a significant degradation of the isolation at high frequency, already observed in the case of an ideal structure. On the other hand, the compliance remains unchanged at high frequency.

5 Conclusion

Fusion of inertial instruments with sensors collocated with the actuators have been studied to increase the feedback control bandwidth of active vibration isolators. Three types of sensors have been considered for the high frequency component of the fusion: a relative motion sensor, an accelerometer and a force sensor. Their impact on the stability and performance have been presented and compared.

The high-frequency fusion with a relative sensor improves the stability but compromises the transmissibility. It can be of interest for stiff suspension with little passive isolation, or for application in which the high-frequency isolation can be sacrificed to improve the stability. However, the flexibility of the support structure must be carefully taken into account for the design of the fusion filter.

The fusion with an accelerometer is an interesting configuration to further increase the loop gain. However, as the accelerometer is not dual to the actuator, this method does not guaranty stability when the isolation stage is mounted on a flexible support.

Finally, the fusion with a force sensor can be used to increase the loop gain with little effect on the compliance and passive isolation, provided that the blend is possible and that no active damping of the flexible modes is required. The results of this investigation will be further investigated (e.g. high frequency sensor noise, multi degree of freedom systems) for application on seismic isolation systems used in Advanced LIGO gravitational wave detectors. They will also be of interest for other applications where high vibration isolation performance is required, like future particle colliders, precise manufacturing machines, or satellite test facilities.

Acknowledgments

The authors gratefully acknowledge the LIGO visitors Program for making possible this collaborative work between the Université Libre de Bruxelles and the LIGO laboratory. LIGO was constructed by the California Institute of Technology and Massachusetts Institute of Technology with funding from the National Science Foundation and operates under cooperative agreement PHY-0107417. The authors also gratefully acknowledge the members of the LIGO Seismic Working Group for their comments and inspiring discussions, and particularly Jeff Kissel for carefully proof-reading the manuscipt and making valuable comments. This document was assigned LIGO Document number LIGO-P1400099.

References

[1] B. Abbott, et al., *Ligo: the laser interferometer gravitational-wave observatory*, Reports on Progress in Physics 72 (7) (2009) 076901.
URL `http://stacks.iop.org/0034-4885/72/i=7/a=076901`

[2] C. Collette, S. Janssens, K. Artoos, A. Kuzmin, P. Fernandez Carmona, M. Guinchard, R. Leuxe, C. Hauviller, *Nano-motion control of heavy quadrupoles for future particle colliders: An experimental validation.*, Nucl. Instrum. Methods Phys. Res., A 643 (EuCARD-PUB-2011-004. 1) (2011) 95–101.

[3] C. Collette, S. Janssens, P. Fernandez-Carmona, K. Artoos, M. Guinchard, C. Hauviller, A. Preumont, *Review: Inertial sensors for low-frequency seismic vibration measurement*, Bulletin of the Seismological Society of America 102 (4) (2012) 1289–1300.

[4] F. Matichard, *et al.*, *LIGO vibration isolation and alignment platforms: an overview of systems, features and performance of interest for the field of precision positioning and manufacturing*, ASPE conference on Control of Precision Systems, 2013.

[5] W. Gevarter, *Basic relations for control of flexible vehicles*, AIAA journal 8 (1970) 666–672.

[6] G. Martin, *On the control of flexible mechanical systems*, Ph.D. thesis, Stanford University (1978).

[7] M. Stieber, *Sensors, actuators, and hyperstability of structures*, no. 10.2514/6, Guidance, Navigation and Control Conference, 1988, pp. 1988–4057.

[8] C. Goh, T. Caughey, *On the stability problem caused by finite actuator dynamics in the collocated control of large space structures*, International journal of control 41 (3) (1985) 787–802.

[9] F. Matichard, *et al.*, *Prototyping, testing, and performance of the two-stage seismic isolation system for advanced ligo gravitational wave detectors*, ASPE conference on Control of Precision Systems, 2010.

[10] F. Matichard, K. Mason, R. Mittleman, B. Lantz, B. Abbott, M. McInnis, A. LeRoux, M. Hillard, C. Ramet, S. Barnum, A. Stein, S. Foley, H. Radkins, J. Kissel, V. Biscans, S. Lhuillier, *Dynamics enhancements of advanced ligo multi-stage active vibration isolators and related control performance improvement*, Proceedings of the 24th Conference on Mechanical Vibration and Noise, Chicago, Illinois, USA, 2012.

[11] J. Spanos, *Control-structure ineraction in precision pointing servo loops*, Journal of Guidance, Control and Dynamics 12 (1989) 256-263.

[12] H. Frahm, *Improved means for damping the vibrations of bodies* (GB190923829A).

[13] J. Ormondroyd, J. Den Hartog, *The theory of damped vibration absorber*, Journal of Applied Mechanics 50 (1929) 7.

[14] J. Yocum, L. Slafer, *Control system design in the presence of severe structural dynamics interactions*, Journal of Guidance, Control and Dynamics 1 (1978) 109–116.

[15] W. Hua, *Low frequency vibration isolation and alignment system for advanced LIGO*, Ph.D. thesis, Stanford University (2005).

[16] G. Hauge, M. Campbell, *Sensors and control of a space-based six-axis vibration isolation system*, Journal of Sound and Vibration 269 (2004) 913–931.

[17] D. Tjepkema, J. Van Dijk, H. M. J. R. Soemers, *Sensor fusion for active vibration isolation in precision equipment*, Journal of Sound and Vibration 331 (4) (2012) 735–749.

[18] M. A. Beijen, D. Tjepkema, J. van Dijk, *Two-sensor control in active vibration isolation using hard mounts*, Control Engineering Practice 26 (0) (2014) 82 – 90.

[19] F. Fleming, *The effect of structure, actuator and sensor on the zeroes of collocated structures*, Ph.D. thesis, Massachusetts Institute of Technology, Cambridge (1990).

[20] D. Tjepkema, *Active hard mount vibration isolation for precision equipment*, Ph.D. thesis, University of Twente (2012).